



In situ metal ion contamination and the effects on proton exchange membrane fuel cell performance

Mark Sulek*, Jim Adams, Steve Kaberline, Mark Ricketts, James R. Waldecker

Ford Motor Company, Research and Advanced Engineering, 2101 Village Road, Dearborn, MI 48121, United States

ARTICLE INFO

Article history:

Received 3 December 2010
Received in revised form 21 January 2011
Accepted 27 January 2011
Available online 2 February 2011

Keywords:

PEM fuel cells
Metal contamination
Membrane degradation
Metal ions
Membrane contamination

ABSTRACT

Automotive fuel cell technology has made considerable progress, and hydrogen fuel cell vehicles are regarded as a possible long-term solution to reduce carbon dioxide emissions, reduce fossil fuel dependency and increase energy efficiency. Even though great strides have been made, durability is still an issue. One key challenge is controlling MEA contamination. Metal ion contamination within the membrane and the effects on fuel cell performance were investigated. Given the possible benefits of using stainless steel or aluminum for balance-of-plant components or bipolar plates, cations of Al, Fe, Ni and Cr were studied. Membranes were immersed in metal sulfide solutions of varying concentration and then assembled into fuel cell MEAs tested in situ. The ranking of the four transition metals tested in terms of the greatest reduction in fuel cell performance was: $\text{Al}^{3+} \gg \text{Fe}^{2+} > \text{Ni}^{2+}, \text{Cr}^{3+}$. For iron-contaminated membranes, no change in cell performance was detected until the membrane conductivity loss was greater than approximately 15%.

© 2011 Elsevier B.V. All rights reserved.

1. Introduction

Automotive fuel cell technology has made significant strides, as evidenced by the number of automakers that have engaged in vehicle demonstration programs and the progress shown in these programs. Although the means of generating hydrogen heavily influence well-to-wheels studies, there is widespread consensus that hydrogen fuel cell vehicles represent one of the better possibilities in the long-term future for reducing carbon dioxide emissions, reducing dependence on fossil fuels, and improving energy efficiency. Like with any technology, fuel cell vehicle commercialization will depend on the ability to match customer expectations regarding performance, range, energy charging time, robustness, durability and cost. While fuel cell vehicles have been shown to meet many of these expectations, degradation and early failure of the proton exchange membrane fuel cell (PEMFC) is still a challenge. Current PEMFC technologies do not meet the required 5000 h (150,000 miles at an average speed of 30 MPH) for normal vehicle operation [1]. The different degradation processes that can lead to failure of the membrane electrode assembly (MEA) within the PEM fuel cell have been well-described in a few recent reviews [2,3].

One key element to fuel cell degradation and decreased cell performance is contamination. The impurities from humidified feed gases and system components can directly enter the MEA, poisoning catalyst sites, impeding proton transport, and inhibiting oxygen transport by decreasing hydrophobicity, all of which cause performance degradation [4]. This paper looks particularly at metal ion contamination within the membrane and the effects on fuel cell performance. While metal ions may be introduced into the fuel cell stack as a consequence of leaching from system components, metal ions may also derive from the increasingly popular use of metal bipolar plates in automotive fuel cell stacks. Metal bipolar plates are being used to meet requirements for manufacturing throughput, cost and volumetric power density. In particular, plates using stainless steel substrates are attractive because of the low cost, high strength, and availability of stainless steel [5]. Metal ions of interest in this study include those that represent most of the composition of stainless steels: iron, nickel and chromium. Aluminum is also studied here since the lower density of aluminum and the low propensity of aluminum cations to catalyze chemical degradation of the membrane [6] could make aluminum a candidate for plate substrates and system components. Because many variations of metal plates and plate coatings or treatments exist [7], the degree and speciation of membrane contaminants will change greatly depending on plate substrate selection, coating composition, and even weld composition. Determining realistic degrees of contamination from many possible plate compositions is beyond the scope of this paper; instead, it is the intention of this paper to select set levels of membrane contamination with the metal cations of interest, and to then

* Corresponding author at: Fuel Cell & Hydrogen Storage Research/R&AE, REC R, Room 1415-1 MD 1170 RIC, Ford Motor Company, 2101 Village Rd., Dearborn, MI 48121, United States. Tel.: +1 313 845 1366; fax: +1 313 621 0646; mobile: +1 313 670 4331.

E-mail address: msulek@ford.com (M. Sulek).

compare the relative amounts of performance loss for those metal cations.

2. Experimental

2.1. Materials

In situ testing was performed using the fuel cell hardware assembly from Fuel Cell Technologies, Inc. The cell consisted of a pair of graphite blocks with 5 cm² machined serpentine flow fields and a pair of gold-plated aluminum end plates. Materials used to fabricate MEAs were DuPont Nafion NRE212CS fuel cell membranes (3 in. × 3 in.), E-Tek gas diffusion electrodes (GDEs) with platinum loading of 5.0 g m⁻² (1.2 in. × 1.2 in.), and gasket material made of class VI medical grade silicone rubber (3 in. × 3 in.). Metal ions used were derived from metal sulfates.

2.2. Procedure

2.2.1. Metal ion contamination of membranes

NRE212CS membranes were placed in beakers containing 1, 5, and 10 ppm metal ion solutions in deionized water. Metals ions solutions used in this study were formed using the hydrated metal sulfates, FeSO₄, NiSO₄, Cr₂(SO₄)₃ and Al₂(SO₄)₃. The membranes were contaminated with metal ions by immersing the membrane in the metal ion solution for 24 h with stirring. The membranes were then removed and rinsed thoroughly. The contaminated membranes were used to fabricate MEAs.

A Metrohm Trace Element Analyzer was used to measure the amount of iron ions absorbed by the membrane. The initial solutions of 10, 5, and 1 ppm Fe²⁺ were measured before the NRE212CS membrane was immersed into metal ion solution. After 24 h, the membranes were removed and placed in a cell for polarization analysis and the remaining solution was collected. The difference between the initial and final metal ion content was used to determine the amount of metal ions absorbed into the membrane.

2.2.2. BOL polarization

The fuel cell was connected to the fuel cell system and conditioned for 24 h with a constant voltage of 0.6 V. After conditioning the cell was operated to record polarization data. The operating conditions used are listed below in Table 1. The air side was fully open to reduce cathode flooding problems and to ensure that the cell performance was not limited by O₂ availability. Only beginning of life (BOL) polarization data was collected.

Table 1
Operating conditions for measuring cell performance.

	Anode	Cathode
Pressure (psig)	10	10
Flow rate (sccm)	300	6340
Humidifier temperature (°C)	70	70
Cell temperature (°C)		70

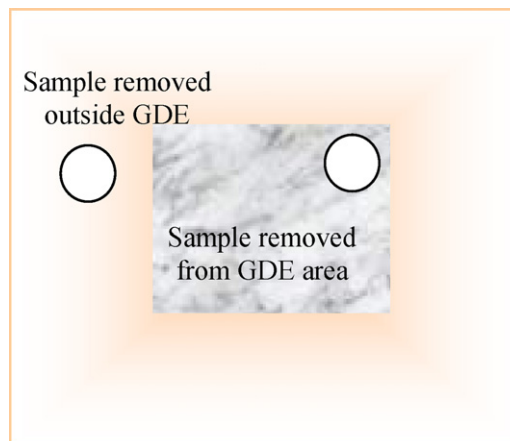


Fig. 1. Membrane areas removed for ToF-SIMS analysis.

After polarization data were recorded, the cell was disassembled and the contaminated membranes were used for time of flight secondary ion mass spectrometry (ToF-SIMS) analysis. A cross-section was taken in two areas for analysis: the region where the GDE layer was positioned over the membrane; and a region that was not covered by GDE, as shown in Fig. 1. Investigation was performed only on the 10 ppm contaminated samples.

3. Results

The baseline BOL polarization data for the NRE212CS membrane without metal ion contamination had an activation region and a linear ohmic region, as shown in Figs. 2–5. No mass transport limited region was observed, as expected, due to the high air flow rate on the cathode side. The performance of the metal ion contaminated membranes was compared to the baseline performance at a cell voltage of 0.6 V. For the baseline membranes, the cell performance was 1.60 A cm⁻² at 0.60 V; at this current den-

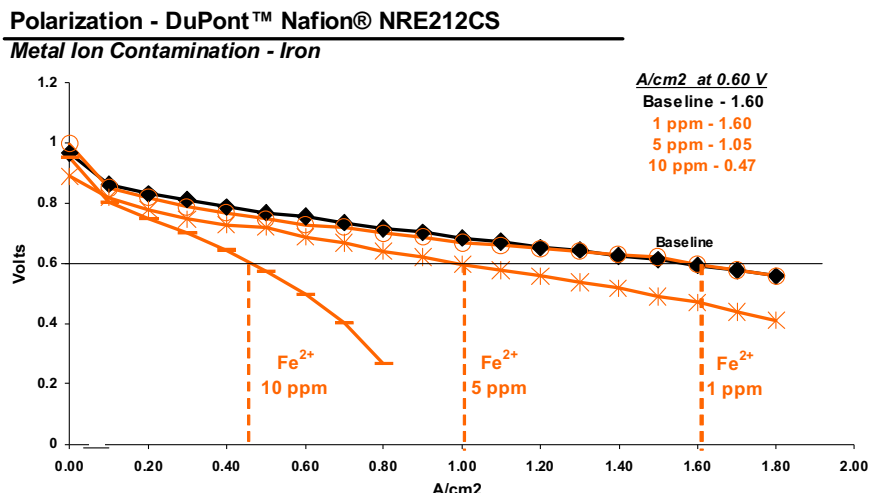


Fig. 2. BOL polarization data for iron contaminated membranes.

Polarization - DuPont™ Nafion® NRE212CS

Metal Ion Contamination - Aluminum

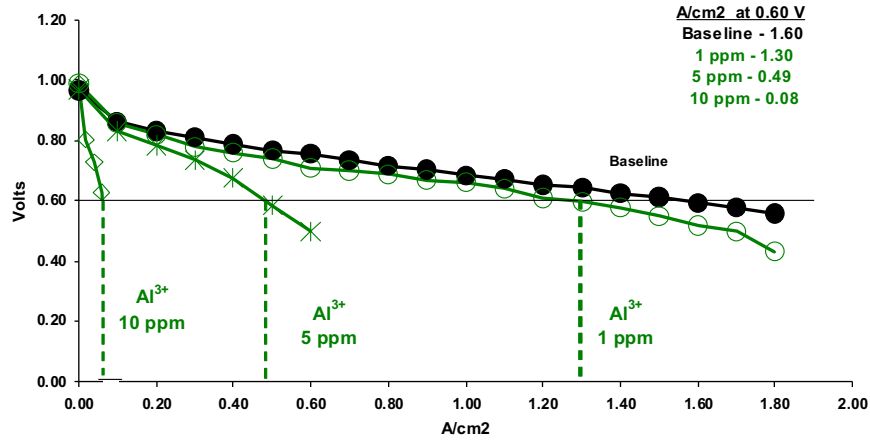


Fig. 3. BOL polarization data for aluminum contaminated membranes.

Polarization - DuPont™ Nafion® NRE212CS

Metal Ion Contamination - Chromium

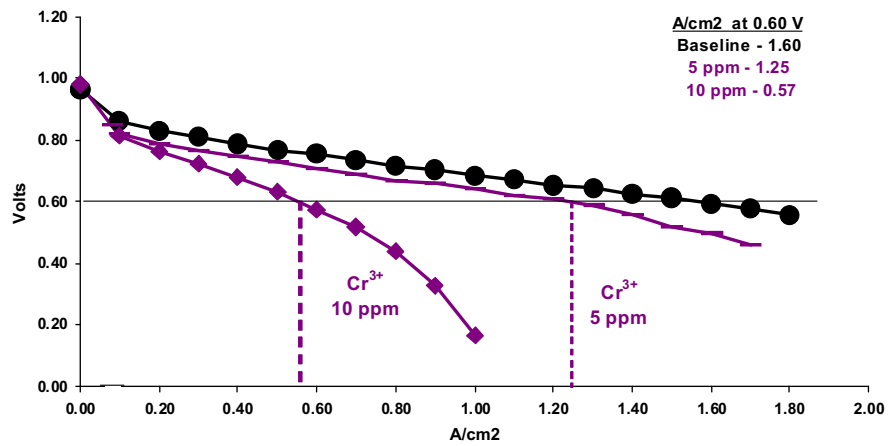


Fig. 4. BOL polarization data for chromium contaminated membranes.

Polarization - DuPont™ Nafion® NRE212CS

Metal Ion Contamination - Nickel

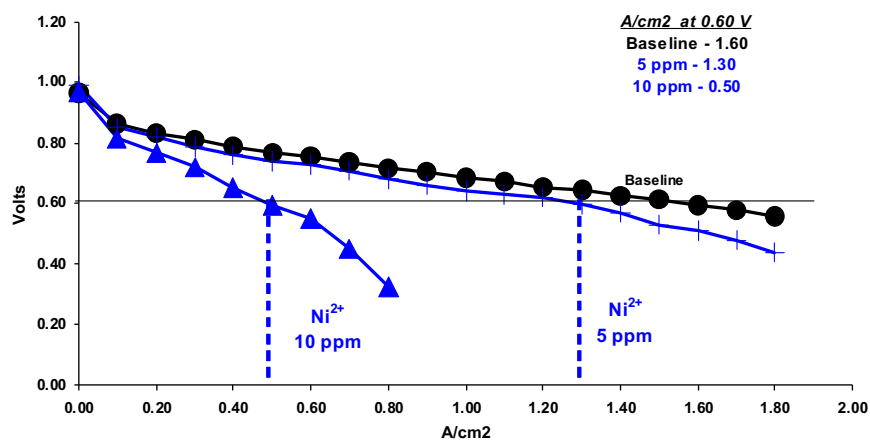


Fig. 5. BOL polarization data for nickel contaminated membranes.

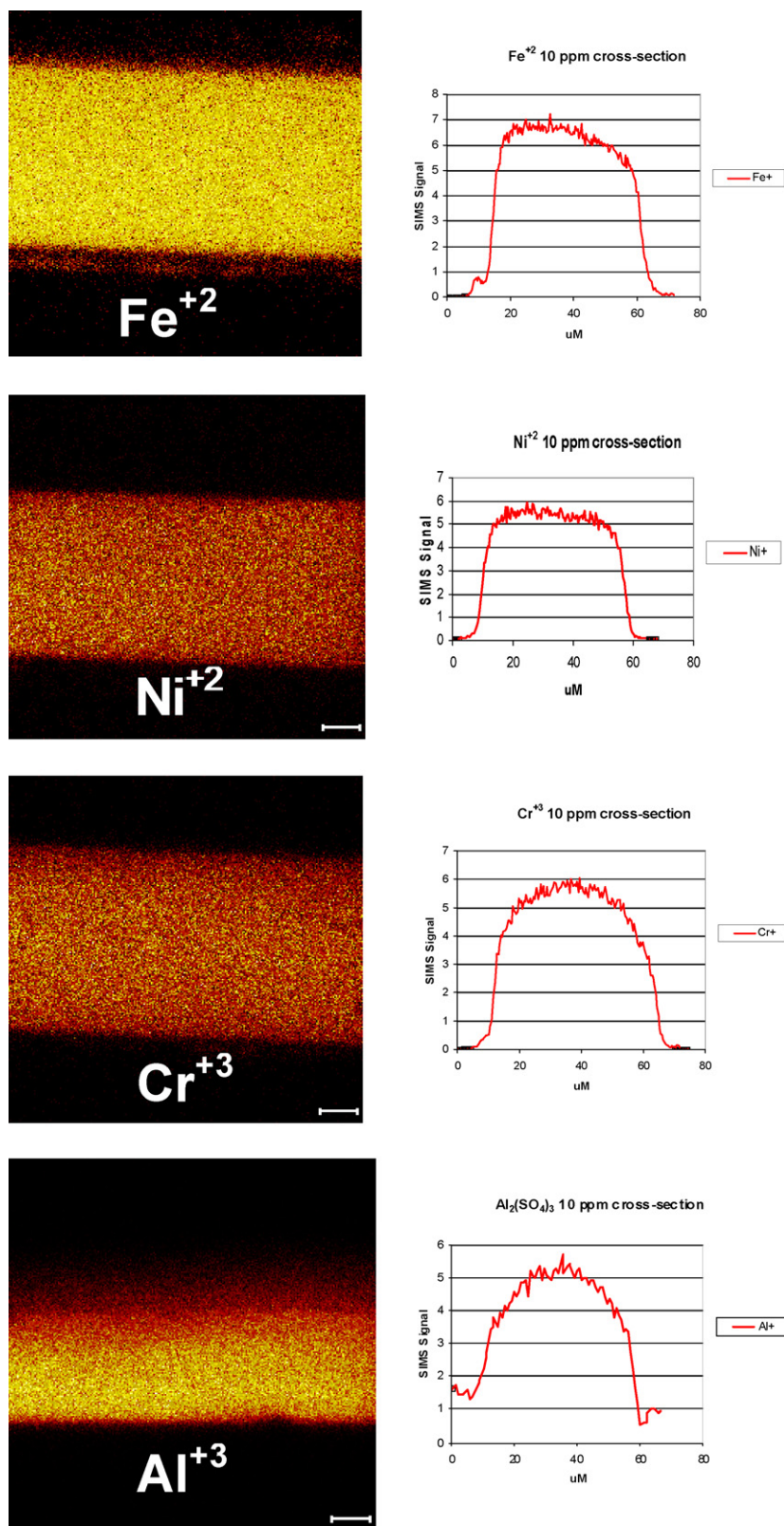


Fig. 6. Time of flight, secondary ion mass spectrometry (ToF-SIMS) metal ion analysis for contaminated membranes.

sity, the air flow rate of 6340 sccm corresponded to a stoichiometry of 110.

The BOL polarization data for NRE212CS membranes contaminated with 1, 5, and 10 ppm iron solutions are shown in Fig. 2. At 1 ppm iron, no loss in cell performance was measured com-

pared to the baseline performance at 0.6 V. At 5 ppm iron, a 34% loss in cell performance was measured, but no mass transport limited region was observed. At 10 ppm iron, a 71% loss in cell performance was measured, and a distinct mass transport limited region in the polarization data was observed.

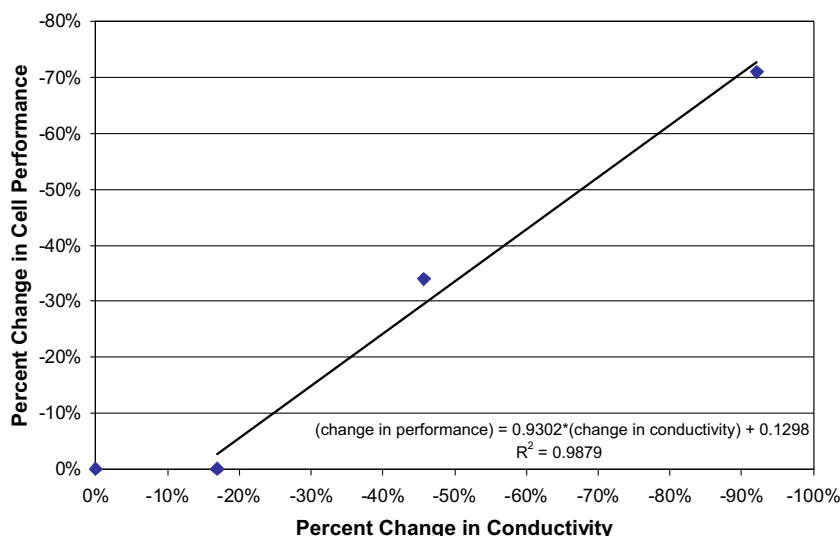


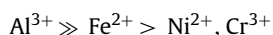
Fig. 7. Effect of change in membrane conductivity on change in cell performance at 0.6 V (for membranes immersed in 1, 5 and 10 ppm Fe solutions).

The BOL polarization data for NRE212CS membranes contaminated with 1, 5, and 10 ppm aluminum solutions are shown in Fig. 3. At 1 ppm aluminum, a 19% loss in cell performance at 0.6 V was measured; the beginnings of a mass transport limited region was observed at the high current densities. At 5 ppm aluminum, a 69% loss in cell performance was measured, and a distinct mass transport limited region was observed. At 10 ppm aluminum, a 95% loss in cell performance was measured.

The BOL polarization data for NRE212CS membranes contaminated with 5 and 10 ppm chromium solutions are shown in Fig. 4. At 5 ppm chromium, a 22% loss in cell performance was measured, but no mass transfer limited region was observed. At 10 ppm chromium, a 64% loss in cell performance was measured, and a distinct mass transport limited region in the polarization data was observed. No data at 1 ppm chromium were collected because the performance at 5 ppm chromium was only slightly reduced compared to the baseline.

The BOL polarization data for NRE212CS membranes contaminated with 5 and 10 ppm nickel solutions are shown in Fig. 5. At 5 ppm nickel, a 19% loss in cell performance was measured, but no mass transport limited region was observed. At 10 ppm nickel, a 69% loss in cell performance was measured, and a distinct mass transport limited region in the polarization data was observed.

The ranking of the four transition metals tested in terms of the greatest reduction in fuel cell performance was as follows:



Aluminum and chromium were anticipated to produce the greatest loss in performance due to their higher valence. However, this hypothesis held true only for aluminum. The reduction in performance produced by nickel and chromium was statistically equivalent at the contamination levels tested. The actual oxidation state of iron and chromium in the solution was not known. For example, ferrous iron can be oxidized to ferric iron by dissolved oxygen in solution. Also, the number of water molecules associated with the cations can vary, which could influence the movement of ions in the membrane. The above two factors may have influenced the impact of each cation on cell performance.

The reason for the development of a mass transport region in the polarization data cannot be known based on the data presented here. One possibility is that the metal ion contamination migrated out of the membrane into the catalyst layer or microporous layer,

where it reduced the hydrophobicity and increased flooding at high current densities.

To determine the distribution of metal ions in the membrane, ToF-SIMS was used as a qualitative tool on membranes contaminated with 10 ppm metal ion solutions. As seen in Fig. 6, all metal ions are dispersed evenly throughout the cross-section tested. The rounding of the corners of the distributions was due to mounting of the sample between two polyethylene sheets, which had a different conductivity than the sample.

The amount of iron absorbed into the membrane was estimated using the trace element analyzer. Iron was chosen because it represents the major potential contaminant present in a fuel cell system. The amount of iron absorbed was determined measuring the difference in the iron solution concentration before and after contaminating the membrane. The data are shown in Table 2. Note that insoluble iron oxide was observed in the iron solutions, probably due to the oxidation of ferrous to ferric iron. The insoluble iron oxide was probably responsible for the difference between the original iron concentration and the measured concentration using the trace element analyzer.

Using the data in Table 2, the amount of iron absorbed into the membrane was calculated. The amount of iron absorbed scales with the initial measured concentrations of iron, as expected. The percentage of sulfonic acid sites bound with iron was also calculated and varied from 1% to 30%. The loss of active sulfonic acid sites produced a change in membrane conductivity of –17% to –92% for the three iron solutions tested.

For membranes immersed in the three iron solutions, the loss of cell performance measured at 0.6 V was compared to the change in membrane conductivity in Fig. 7. No change in cell performance was detected until the membrane conductivity loss was greater than approximately 15%, suggesting that some metal ion contam-

Table 2

Results from trace element analyzer of iron ions absorbed into the membrane.

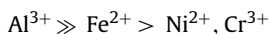
Original Fe ²⁺ conc. (ppm)	1	5	10
Initial measured Fe ²⁺ conc. (ppm)	0.37	3.02	5.97
Final measured Fe ²⁺ conc. (ppm)	0.04	0.18	0.45
Solution volume (ml)	500	500	750
Fe ²⁺ absorbed into membrane (mg Fe ²⁺ g ⁻¹ membrane)	0.27	2.3	6.7
Percent SO ₃ ⁻ sites bound with Fe ²⁺	1	10	30

ination can be tolerated with respect to cell performance, or that metal cation-related ohmic losses were within the experimental error associated with cell assembly. However, the above statement refers only to the particular failure mode of metal cations displacing protons at sulfonic acid group in ionomeric phases. The ability of some metal ions, such as Fe^{2+} , to catalyze Fenton-type degradation reactions should also be considered [2]. Above approximately a 15% loss in conductivity, the cell performance degrades in a linear manner with a slope near unity.

4. Conclusion

There are many reasons why state-of-the-art PEMFCs still present durability concerns, but one major contribution to fuel cell degradation is contamination. Impurities can enter from humidified reactant gas feeds and coolant, as well as from stack components such as bipolar plates. Metals cations bind with high affinity to sulfonic acid sites in the membrane and catalyst layer ionomer, reducing the protonic conductivity and therefore fuel cell performance.

The ranking of the four transition metals tested in terms of the greatest reduction in fuel cell performance was as follows:



All metal ions were dispersed evenly throughout the cross-section tested. For iron-contaminated membranes, no change in cell performance was detected until the membrane conductivity loss was greater than approximately 15%, suggesting that some metal ion contamination may be tolerated with respect to cell performance, or that performance loss at low contamination is within error of cell assembly repeatability. Above approximately a 15% loss in conductivity, the cell performance degrades in a linear manner with a slope near unity.

References

- [1] FreedomCAR Fuel Cell Roadmap, http://www.uscar.org/commands/files-download.php?files_id=81.
- [2] R. Borup, J. Meyers, B. Pivovar, Y.S. Kim, R. Mukundan, N. Garland, D. Myers, M. Wilson, F. Garzon, D. Wood, P. Zelenay, K. More, K. Stroh, T. Zawodzinski, J. Boncella, J.E. McGrath, M. Inaba, K. Miyatake, M. Hori, K. Ota, Z. Ogumi, S. Miyata, A. Nishikata, Z. Siroma, Y. Uchimoto, K. Yasuda, K. Kimijima, N. Iwashita, *Chem. Rev.* 107 (10) (2007) 3904–3951.
- [3] J. Wu, X.Z. Yuan, J.J. Martin, H. Wang, J. Zhang, J. Shen, S. Wu, W. Merida, *J. Power Sources* 184 (2008) 104–119.
- [4] X. Cheng, Z. Shi, N. Glass, L. Zhang, J. Zhang, D. Song, Z. Liu, H. Wang, J. Shen, *J. Power Sources* 165 (2007) 739–756.
- [5] A. Kumar, M. Ricketts, S. Hirano, *J. Power Sources* 195 (2010) 1401–1407.
- [6] A. Pozio, R.F. Silva, M. De Francesco, L. Giorgi, *Electrochim. Acta* 48 (2003) 1543–1549.
- [7] H. Tawfik, Y. Hung, D. Mahajan, *J. Power Sources* 163 (2007) 755–767.